Computational Materials Science 207 (2022) 111240

Contents lists available at ScienceDirect

Computational Materials Science

journal homepage: www.elsevier.com/locate/commatsci

Assessing Mg–Sc–(rare earth) ternary phase stability via constituent binary cluster expansions

Anna Soper [a,*], Adam L. Shaw [a,b], Patrick L.J. Conway [c], Gregory S. Pomrehn [d], Michael Ferry [c], Lori Bassman [a], Aurora Pribram-Jones [e], Kevin J. Laws [c]

[a] Department of Engineering, Harvey Mudd College, Claremont, CA 91711, USA
[b] Department of Physics, Mathematica, and Astronomy, California Institute of Technology, Pasadena, CA 91125, USA
[c] School of Materials Science and Engineering, UNSW Sydney, Sydney, NSW 2052, Australia
[d] The Boeing Company, Seattle, WA 98108, USA
[e] School of Natural Sciences, University of California, Merced, CA 95343, USA

ARTICLE INFO

Keywords:
Cluster expansion
Magnesium alloys
Rare-earth metals

ABSTRACT

The disordered Mg–Sc body-centered cubic (bcc) phase is both lightweight and strong; however, the system is impractical for general industrial use due to the high cost of scandium. We propose a computationally efficient metric that assesses ternary rare earth element additions that may stabilize the bcc phase at lower Sc concentrations. We find that the bcc phase is stabilized by the ternary addition of Y or Er, but not by La, Ce, or Nd, and we validate these predictions by experimental production and characterization of Mg–Sc–(Y,Er,Nd) alloys. The results suggest a computationally efficient method to anticipate integration of ternary elements into binary systems using cluster expansions of constituent binaries.

1. Introduction

Magnesium-based alloys have received increased attention as demand for lightweight materials has grown in the automotive, aerospace and biomedical industries [1–5]. Both computational and experimental efforts have attempted to identify possible alloy partners for Mg to enhance desirable mechanical properties while maintaining a low overall mass density [6–9]. One avenue currently being explored is Mg–rare earth (RE) alloys, which are strong, ductile, and low density [10–15]. Of these, the Mg–Sc binary system fosters a particularly interesting high temperature, disordered body-centered cubic (bcc) phase that exhibits high strength, ductility, and creep resistance [9,16–19]. This so-called β-phase extends across a wide composition range, with a minimum equilibrium temperature of 480 °C at ~25 at.% Sc (Fig. 1) [20], but it can be realized via heat treating at 700 °C and water quenching. At equilibrium temperatures below 480 °C, the β-phase begins to order, evolving into the brittle MgSc B2 phase, while for lower Sc concentrations, a two-phase field forms, comprised of the hexagonal close packed (hcp) α-Mg phase and the MgSc B2 phase; neither necessarily promotes a desirable combination of ductility and strength [21,22].

The β-phase can be retained for lower Sc concentrations via the substitution of ternary or quaternary elements in low concentrations. Previously, we have experimentally shown that the β-phase can be stabilized via the substitution of ~5 at.% Y for Sc [23], and we now seek to determine if other ternary REs can produce similar behavior. Since Sc is at least an order of magnitude more expensive than any other rare earth element in this study, substitutions that reduce the required concentration of Sc by even a few percent may drastically increase the practicality of these materials for industrial applications.

Several recent first principles computational simulations have been dedicated to investigating the mechanical and phase properties of Mg–Sc [8,12,13,24,25]. However there are few studies on the phase behavior of ternary (or higher order) Mg–Sc-based alloys, due in part both to the combinatorial complexity of exploring higher order composition spaces and to the challenge of properly simulating multi-component disordered alloy behavior.

Related work in the high entropy alloy community relies on a variety of methods such as special quasirandom structures (SQS) [26], the coherent potential approximation (CPA) [27], small sets of ordered structures (SSOS) [28], and direct interrogation of lattice cluster expansions (CE) via Monte Carlo integration from a high temperature limit [29]. However, all of these methods show drawbacks: necessarily large supercells (SQS), insensitivity to local lattice distortions (CPA), a limited basis set (SSOS), and inefficient scaling for ternary or higher order alloys (CE).

* Corresponding author.
E-mail address: asoper@hmc.edu (A. Soper).

https://doi.org/10.1016/j.commatsci.2022.111240
Received 29 October 2021; Received in revised form 23 January 2022; Accepted 26 January 2022
Available online 25 February 2022

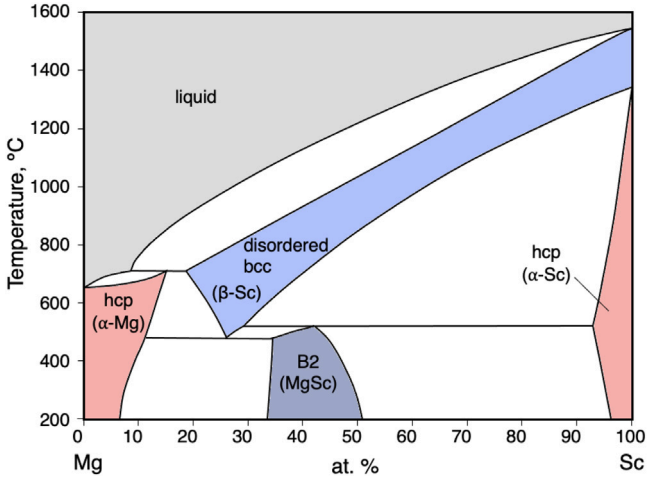

Fig. 1. Mg–Sc binary phase diagram. The desired disordered bcc β phase first forms at 480 °C and 25 at.% Sc. In the neighboring two phase regions, the alloy segregates with nearly pure Mg or Sc on the hcp lattice.
Source: Adapted with permission from Ref. [20].

In this paper, we address the issue of predicting RE integration into the disordered β-phase by developing a heuristic using only efficiently generated constituent binary cluster expansions. At elevated temperatures, Mg–Sc either forms the desired disordered bcc β phase or segregates with nearly pure Mg or Sc on the hcp lattice (Fig. 1). Thus, we build our heuristic on the premise that a RE addition will integrate into the β-phase when the favorability of bcc and hcp phases in Mg–RE and Sc–RE binaries mimics that of Mg–Sc. We calculate lattice cluster expansions for a number of Mg–RE and corresponding Sc–RE alloys and employ our model to predict the β-stabilizing power of these RE additions to the Mg–Sc binary system. While this work, which is based on the sets of constituent binaries for each Mg–Sc–RE ternary alloy candidate, is not able to fully capture the ternary behavior, the results are directly compared against experimentally produced alloys with good agreement. This method not only demonstrates the ability to efficiently screen plausible Mg–Sc–RE combinations, but also has the potential to be adapted for use with other alloy systems.

2. Computational methods

The cluster expansion models in this study are fit using calculated zero-temperature energies of ordered structures with up to 16 atoms per unit cell. These energies are calculated explicitly with density functional theory (DFT) [30] using the Vienna Ab Initio Simulation Package (VASP) [31,32] under the Perdew–Burke–Ernzerhof (PBE) [33] generalized gradient approximation. Projector augmented wave (PAW) pseudopotentials supplied by VASP are used with a plane wave energy cutoff of 450 eV [34]. Sampling is performed on a Γ-centered Monkhorst–Pack k-mesh composed of approximately 8000 k-points per reciprocal atom [35]. Formation energies for binary alloys are calculated relative to the pure hcp phases.

A cluster expansion is fit for each Mg–RE and Sc–RE binary alloy system in this study using software tools from the Alloy-Theoretic Automated Toolkit (ATAT) [36,37]. Formally, we write the system Hamiltonian for a given lattice (bcc, hcp) as

$$H(\vec{\sigma}) = \sum_{\alpha} J_{\alpha} m_{\alpha} \Phi_{\alpha}(\vec{\sigma}) \tag{1}$$

where the sum extends over all symmetrically distinct clusters α. We truncate the size of the clusters to include a maximum of four lattice sites, but place no bound on the cluster radius and instead allow ATAT to choose the most energetically relevant clusters. The set of $\Phi_{\alpha}(\vec{\sigma})$ are the cluster correlation functions for a given configuration, $\vec{\sigma}$, of atomic species on the crystal lattice, with m_{α} being the number of symmetrically equivalent clusters in the orbit of cluster α. The correlation functions are calculated using occupation variables of +1 for Mg or Sc and −1 for the RE element. The set of J_{α} are the effective cluster interactions (ECI), coefficients representing how each cluster affects the total energy of the lattice arrangement [36]. These coefficients are fit using DFT-calculated energies of ordered configurations (Fig. 2). Each expansion is considered converged when it correctly reproduces all ground state structures (as calculated by DFT) with an accuracy of 0.01 eV/atom. The cluster expansions are fit with 50 to 320 DFT-calculated structure energies in order to meet this requirement.

3. Calculations and results

Fig. 2 shows the energies of bcc and hcp zero temperature ground state structures for Mg–RE and Sc–RE binaries. The Mg–RE binaries have lower bcc energies at intermediate compositions, as desired for the stabilization of the bcc β-phase. Although the Sc–RE binaries do not exhibit this same pattern, the presence of bcc metastable mixed states with lower energies than the bcc pure structures suggests that bcc stabilization may be possible in combination with Mg–RE alloys.

We seek REs that can serve as a partial substitute for Sc in the Mg–Sc β-phase. To infer the behavior of the ternary Mg–Sc–RE alloys without having to fit a cluster expansion for each ternary combination, we develop a heuristic based on cluster expansion models of the constituent binaries. We propose that a RE addition will integrate into the β-phase when the favorability of bcc and hcp phases in Mg–RE and Sc–RE binaries mimics that of Mg–Sc. Such a metric cannot be deduced directly from binary phase diagrams because of the formation of intermetallics that obscure the crystal structures of interest.

To isolate properties relevant to integration with the Mg–Sc disordered bcc β-phase, we look at the relative favorability of disordered and segregated atomic arrangements on the bcc and hcp lattices. To capture these energetics, we define

$$\mathcal{J} = E_{\text{disordered}} - E_{\text{segregated}} \tag{2}$$

for each constituent Mg–RE and Sc–RE binary on the bcc ($\mathcal{J}_{\text{bcc}}$) and hcp ($\mathcal{J}_{\text{hcp}}$) lattices, where E is the zero temperature formation energy of the specified configuration. As shown in Fig. 1, at elevated temperatures, the Mg–Sc system tends to form either a single disordered bcc phase or segregate into a two-phase region where nearly pure Mg or Sc sits on the hcp lattice. This behavior is captured in the $\mathcal{J}_{\text{bcc}}$ and $\mathcal{J}_{\text{hcp}}$ of the Mg–Sc system. At compositions where the desired disordered low Sc bcc phase forms $\mathcal{J}_{\text{bcc}} < 0$ and $\mathcal{J}_{\text{hcp}} > 0$, indicating that a single disordered phase is favored only on the bcc lattice. Translating this into a metric, we propose that a given RE will favor integration into the disordered bcc beta-phase if both of the constituent Mg–RE and Sc–RE binaries mimic this behavior of $\mathcal{J}_{\text{bcc}} < 0$ and $\mathcal{J}_{\text{hcp}} > 0$. While this metric is not designed to predict ternary phase behavior, it serves as an effective guide for narrowing down plausible ternary combinations beyond what can be deduced from constituent binary phase diagrams because it is able to quantify the energetics of bcc and hcp phases in all relevant parts of the Mg–RE and Sc–RE composition spaces.

To obtain the segregated and disordered structure energies required for the metric, we calculate converged Mg–RE and Sc–RE cluster expansion fits for a number of different REs. We calculate generalized cluster correlation functions for disordered and segregated structures and use them in the cluster expansions to obtain the corresponding energies. The cluster expansion Hamiltonian is fit using zero temperature DFT calculations, and in constructing the metric $\mathcal{J}$, we explicitly recast the energetics into a largely temperature-independent form. For the disordered structures, energies are calculated under a mean field approximation, which is valid at finite temperatures for systems with sufficient configurational entropy. For the segregated structures, energies are calculated under the assumption of complete separation of

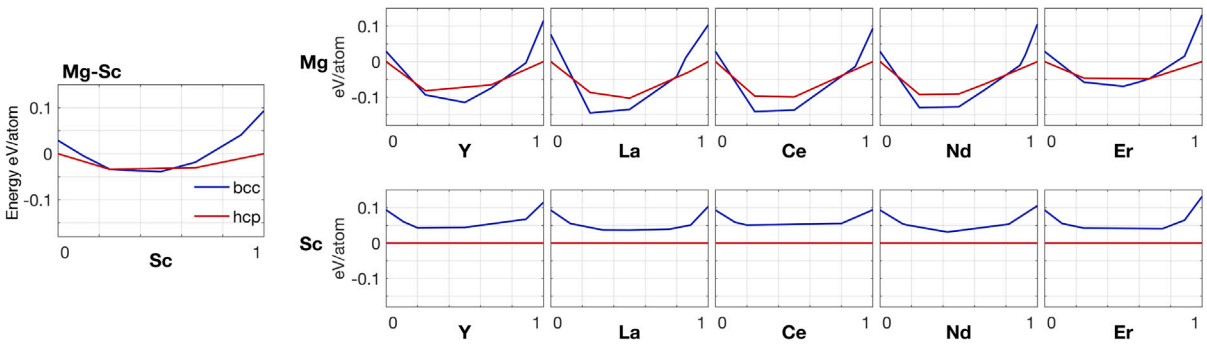

Fig. 2. Zero temperature convex hulls showing the bcc and hcp ground states for several Mg–RE and Sc–RE binaries. Horizontal axes indicate the atomic fractions of RE elements, and all formation energies are shown relative to the pure hcp structures. The bcc lattice is stabilized at intermediate compositions for all Mg–RE pairs but is only ever metastable for Sc–RE systems.

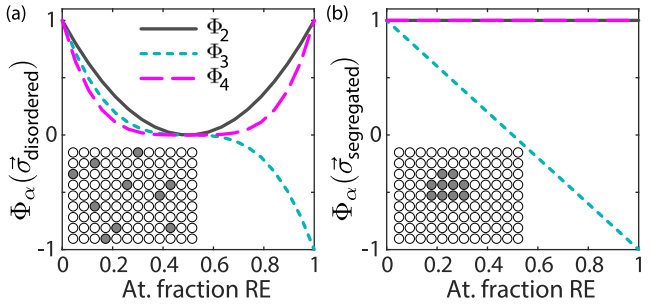

Fig. 3. (a) Pair, triplet and quadruplet cluster correlations as a function of atomic fraction RE for (a) a disordered structure and (b) a segregated structure. The inset lattices are simple two-dimensional representations of our definition of disordered and segregated structures. Occupation variables of +1 and −1 are used for Mg (or Sc) (white circles) and RE (grey circles), respectively.

atomic species, and thus there is no configurational entropy to lead to temperature dependence.

In the limits of complete disorder and segregation on the bcc and hcp lattices, conceptually illustrated by the inset lattices in Fig. 3, the cluster correlation functions become well defined functions of composition, allowing us to calculate the energies of such orderings. For a completely disordered binary structure, the correlation functions are the same as those under the mean field approximation [38]. As shown in Fig. 3a, the mean field correlation function for a cluster of N lattice sites corresponds to an Nth order polynomial. For the segregated lattice (Fig. 3b), we approximate the correlation functions in the limit of a large number of atoms, where the clusters spanning the boundary between Mg (or Sc) and RE regions have a vanishingly small contribution to the correlation function. Ignoring these, we are left with contributions from clusters in regions of pure Mg (or Sc) and pure RE. Recall that the occupation variables for Mg (or Sc) and RE are +1 and −1 respectively. Therefore in a RE region, clusters containing an even number of lattice sites have an occupation product of +1 while clusters containing an odd number of lattice sites have an occupation product of −1. Adding the contributions from clusters in the pure Mg (or Sc) and pure RE regions, the correlation functions become either constant (for even clusters) or linear (for odd clusters) functions of composition.

We use these correlation functions as the $\boldsymbol{\Phi}_\alpha(\vec{\sigma})$ in the cluster expansion Hamiltonian (Eq. (1)) to determine the energies of maximally disordered and maximally segregated structures. As in Eq. (1),

$$E_{\text{segregated}} = \sum_\alpha J_\alpha m_\alpha \boldsymbol{\Phi}_\alpha(\vec{\sigma}_{\text{segregated}}) \tag{3}$$

and

$$E_{\text{disordered}} = \sum_\alpha J_\alpha m_\alpha \boldsymbol{\Phi}_\alpha(\vec{\sigma}_{\text{disordered}}) \tag{4}$$

Table 1
Calculated $\mathcal{J}_{\text{bcc}}$ and $\mathcal{J}_{\text{hcp}}$ for the cluster-expanded Mg–RE and Sc–RE binaries at a composition of 85 at.% Mg, 10 at.% Sc and 5 at.% RE. We maintain the RE atomic percentage when mapping the ternary composition on to the constituent Mg–RE and Sc–RE compositions. For each lattice (bcc and hcp), negative (grey) values indicate that a disordered single-phase is favored while positive (white) values indicate that two-phase segregation is favored. The stability criterion for bcc β-phase stability is $\mathcal{J}_{\text{bcc}} < 0$ and $\mathcal{J}_{\text{hcp}} > 0$, achieved only by the Mg–Sc–Y and Mg–Sc–Er alloy systems.

	$\mathcal{J}_{\text{bcc}}$ (eV/atom)	$\mathcal{J}_{\text{hcp}}$ (eV/atom)	β-phase stability
Mg–Y	−0.009	0.006	✓
Sc–Y	−0.005	0.012	
Mg–Er	−0.003	0.009	✓
Sc–Er	−0.010	0.009	
Mg–Nd	−0.023	−0.003	✗
Sc–Nd	−0.003	0.018	
Mg–La	−0.027	−0.019	✗
Sc–La	−0.004	0.021	
Mg–Ce	−0.019	−0.012	✗
Sc–Ce	0.002	0.025	

These energies are then used in Eq. (2) to calculate the overall $\mathcal{J}$ with up to 10 at.% RE. The criteria of $\mathcal{J}_{\text{bcc}} < 0$ and $\mathcal{J}_{\text{hcp}} > 0$ allow us to identify Mg–Sc–RE systems where the bcc solid solution is stabilized for small RE additions. Note that RE integration into the β-phase is indicated by only the signs of the $\mathcal{J}$ and not their numerical magnitudes.

Table 1 summarizes the calculated $\mathcal{J}$ for the candidate Mg–RE and Sc–RE alloys on both lattices. The results are shown for the composition 85 at.% Mg, 10 at.% Sc and 5 at.% RE; however the β-phase stability conclusions remain unchanged for all RE elements over the entire composition range of interest (1–10 at.% RE, 5–15 at.% Sc, and 75–90 at.% Mg). We first consider the Mg–RE binaries, as the higher concentration of Mg makes their contributions the leading order effect. Only two REs satisfy the binary stability criterion of positive $\mathcal{J}_{\text{bcc}}$ and negative $\mathcal{J}_{\text{hcp}}$: Mg–Y and Mg–Er. To strengthen this result, we can look to the Sc–RE cluster expansions, each of which enters as a lower energy correction. We see that the $\mathcal{J}$ for Sc–Y and Sc–Er support the results obtained for Mg–Y and Mg–Er while all other RE candidates were previously eliminated by the negative Mg–RE $\mathcal{J}_{\text{hcp}}$.

4. Discussion

We produced physical samples of Mg–Sc–Y, Mg–Sc–Er, and Mg–Sc–Nd via induction melting, followed by heat treating at 700 °C for 1 h and water quenching. The phase behavior of the samples was then analyzed with x-ray diffraction and energy dispersive x-ray spectroscopy. A full description of the methods can be found in Ref. [39]. Scanning

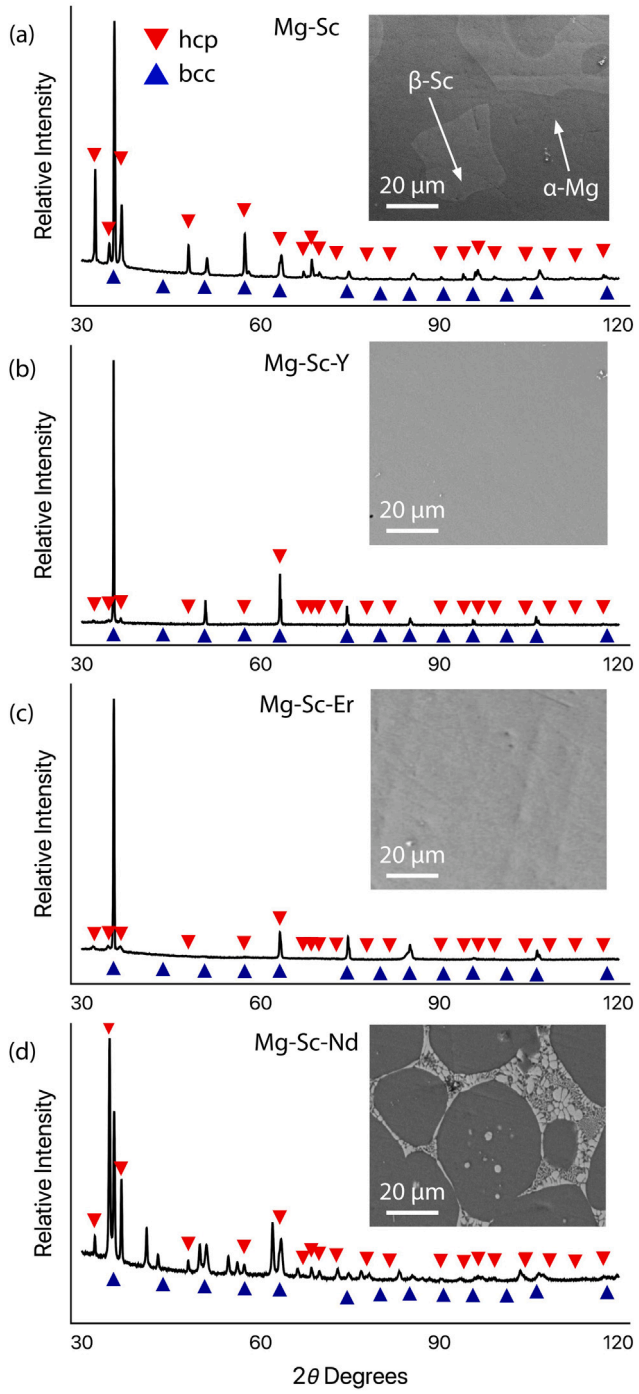

Fig. 4. X-ray diffraction (XRD) traces and scanning electron microscope (SEM) micrographs of (a) a $Mg_{84.8}Sc_{15.2}$ binary, showing the co-existence of both bcc and hcp phases, (b) a $Mg_{82.3}Sc_{14.3}Y_{3.4}$ ternary, confirming the existence of only a bcc phase, (c) a $Mg_{79.4}Sc_{19.0}Er_{1.6}$ ternary, showing only a bcc phase, and (d) a $Mg_{76.7}Sc_{19.5}Nd_{3.8}$ ternary, showing two-phase separation between bcc and hcp lattices, in addition to Mg_3Nd intermetallic formation due to incipient melting during alloy formation. Alloys with higher Nd content (up to 5.9% was produced) also show this phase segregation. Note that the Mg–Sc–Er XRD trace exhibits preferential orientation in the (110) plane. This results in the peaks from other planes being comparatively smaller, however all expected peaks are still detected and included in the Rietveld refinement and determination of the lattice. All SEM micrographs and XRD traces shown are for samples that have been heat treated at 700 °C and water quenched.
Source: Figures adapted (XRD data replotted, SEM images cropped) with permission from Refs. [23,39].

electron micrographs of heat-treated samples shown in Fig. 4 show a single bcc β-phase in Mg–Sc–Y and Mg–Sc–Er, as our developed metric predicts. The Mg–Sc–Nd sample, however, does not show stabilization of a single-phase solid solution, but instead shows separation into a complicated multi-phase microstructure. Thus our model is in good agreement with the experimentally tested Mg–Sc–Y, Mg–Sc–Er and Mg–Sc–Nd ternary alloys.

While the β-phase is stabilized in Mg–Sc–Er at a lower Sc concentration (~19 at.% Sc) than for the Mg–Sc binary (~21 at.% Sc), it still requires more Sc than Mg–Sc–Y (~14 at.% Sc). All percentages have been determined by experiment, where samples with smaller concentrations of Sc exhibited phase segregation [39]. Thus while Er could be a good first step towards reducing the cost of the β-phase bcc alloy, it is not as effective at reducing the needed Sc and hence not as economical as Y. Further, as shown in Table 1, La and Ce (both less expensive than Y) are predicted to be poor β-stabilizers, suggesting Y may be the most attractive option possible for a RE ternary β-stabilizer.

Just as the addition of the ternary Y reduces the necessary concentration of Sc, it is likely the addition of further quaternary or quinary elements to the Mg–Sc–Y system may have a more significant effect. For a first approximation, the binary results from Table 1 can still be used, suggesting a combination of Y and Er may act as a good β-stabilizer in Mg–Sc–Y–Er, though this has not yet been tested experimentally.

5. Conclusion

The bcc β-phase of Mg–Sc has desirable mechanical properties, but is only stable either far above room temperature or for uneconomical Sc concentrations. Additions of low concentrations of rare earth elements, such as Y, can reduce the Sc concentration required for β-stabilization, and thus may make these alloys more accessible to industry applications. An initial set of five RE elements was chosen in part due to the fact that their binary Mg–RE phase diagrams contain the disordered bcc β-phase. Our metric allows us to further narrow down this set of potential RE additions by probing the relative favorability of phases beyond what can be determined from constituent binary phase diagrams. The predictions for Y, Er, and Nd are confirmed by experiment. This computational metric, derived from the cluster expansions of constituent binary alloys, can quickly make predictions for other ternary candidates and can be used to guide experimental fabrication of ternary Mg–Sc–RE alloys in the future. With suitable alterations, the model can be expanded to describe alloys that are non-dilute or do not fit the phase constraints of the Mg–Sc system.

CRediT authorship contribution statement

Anna Soper: Methodology, Formal analysis, Writing – original draft, Writing – review & editing. **Adam L. Shaw:** Conceptualization, Methodology, Software, Investigation, Writing – original draft. **Patrick L.J. Conway:** Investigation, Formal analysis. **Gregory S. Pomrehn:** Methodology, Writing – original draft. **Michael Ferry:** Supervision, Resources. **Lori Bassman:** Writing – review & editing, Supervision, Funding acquisition. **Aurora Pribram-Jones:** Methodology, Writing – review & editing. **Kevin J. Laws:** Resources, Writing – review & editing, Supervision.

Declaration of competing interest

The authors declare that they have no known competing financial interests or personal relationships that could have appeared to influence the work reported in this paper.

Acknowledgments

We acknowledge Jonas Kaufman for insightful conversations and Dr. Caitlin Healy for assistance with XRD analysis. We recognize the financial support of the Jude and Eileen Laspa Fellowship in Applied Mechanics at Harvey Mudd College and the National Science Foundation (OISE-1559403). We appreciate the assistance and support of the UNSW Sydney School of Materials Science and Engineering and Dr. Karen Privat for technical assistance and use of facilities at the Electron Microscope Unit within the Mark Wainwright Analytical Centre at UNSW Sydney. A.P.J. recognizes support by Department of Energy grant number DE-SC0019053. This work used the Extreme Science and Engineering Discovery Environment (XSEDE), which is supported by National Science Foundation grant number ACI-1053575. The authors acknowledge the Texas Advanced Computing Center (TACC) at the University of Texas at Austin for providing high performance computing resources that have contributed to the research results reported within this paper. Fig. 1 adapted by permission from Springer Nature: Elsevier, Bulletin of Alloy Phase Diagrams, *The Mg-Sc (Magnesium-Scandium) system*, A. A. Nayeb-Hashemi and J.B. Clark, 1986. Parts of Fig. 4 are adapted by permission from Springer Nature: Springer International Publishing, Magnesium Technology 2017, *Stabilisation of disordered bcc phases in magnesium-rare earth alloys*, P.L.J. Conway, et al.©The Minerals, Metals & Materials Society, 2017.

References

[1] M.K. Kulekci, Magnesium and its alloys applications in automotive industry, Int. J. Adv. Manuf. Technol. 39 (9) (2008) 851–865, http://dx.doi.org/10.1007/s00170-007-1279-2.

[2] L. Ren, L. Fan, M. Zhou, Y. Guo, Y. Zhang, C.J. Boehlert, G. Quan, Magnesium application in railway rolling stocks: A new challenge and opportunity for lightweighting, Int. J. Lightweight Mater. Manuf. 1 (2) (2018) 81–88, http://dx.doi.org/10.1016/j.ijlmm.2018.05.002.

[3] J. Hirsch, T. Al-Samman, Superior light metals by texture engineering: Optimized aluminum and magnesium alloys for automotive applications, Acta Mater. 61 (3) (2013) 818–843, http://dx.doi.org/10.1016/j.actamat.2012.10.044.

[4] G.S. Cole, A.M. Sherman, Light weight materials for automotive applications, Mater. Charact. 35 (1) (1995) 3–9, http://dx.doi.org/10.1016/1044-5803(95)00063-1.

[5] J. Liu, Y. Lin, D. Bian, M. Wang, Z. Lin, X. Chu, W. Li, Y. Liu, Z. Shen, Y. Liu, Y. Tong, Z. Xu, Y. Zhang, Y. Zheng, In vitro and in vivo studies of Mg-30Sc alloys with different phase structure for potential usage within bone, Acta Biomater. 98 (2019) http://dx.doi.org/10.1016/j.actbio.2019.03.009.

[6] W. Xu, N. Birbilis, G. Sha, Y. Wang, J.E. Daniels, Y. Xiao, M. Ferry, A high-specific-strength and corrosion-resistant magnesium alloy, Nature Mater. 14 (2015) 1229–1235, http://dx.doi.org/10.1038/nmat4435.

[7] K. Kainer, F. von Buch, Magnesium - Alloys and Technology, Wiley-VCH Verlag GmbH & Co. KGaA, 2003, http://dx.doi.org/10.1002/3527602046.ch1.

[8] R.H. Taylor, S. Curtarolo, G.L.W. Hart, Guiding the experimental discovery of magnesium alloys, Phys. Rev. B 84 (8) (2011) 084101, http://dx.doi.org/10.1103/PhysRevB.84.084101.

[9] Y. Ogawa, D. Ando, Y. Sutou, K. Yoshimi, J. Koike, Determination of α/β phase boundaries and mechanical characterization of Mg-Sc binary alloys, Mater. Sci. Eng. A 670 (2016) 335–341, http://dx.doi.org/10.1016/j.msea.2016.06.028.

[10] S. Tekumalla, S. Seetharaman, A. Almajid, M. Gupta, Mechanical properties of magnesium-rare earth alloy systems: A review, Metals 5 (1) (2015) 1–39, http://dx.doi.org/10.3390/met5010001.

[11] L.L. Rokhlin, Advanced Magnesium Alloys with Rare-Earth Metal Additions, Springer Netherlands, Dordrecht, 1998, http://dx.doi.org/10.1007/978-94-015-9068-6_58, Publication Title: Advanced Light Alloys and Composites.

[12] A.R. Natarajan, A. Van der Ven, A unified description of ordering in HCP Mg-RE alloys, Acta Mater. 124 (Supplement C) (2017) 620–632, http://dx.doi.org/10.1016/j.actamat.2016.10.057.

[13] A. Issa, J.E. Saal, C. Wolverton, Physical factors controlling the observed high-strength precipitate morphology in Mg–rare earth alloys, Acta Mater. 65 (Supplement C) (2014) 240–250, http://dx.doi.org/10.1016/j.actamat.2013.10.066.

[14] K. Hantzsche, J. Bohlen, J. Wendt, K.U. Kainer, S.B. Yi, D. Letzig, Effect of rare earth additions on microstructure and texture development of magnesium alloy sheets, Scr. Mater. 63 (7) (2010) 725–730, http://dx.doi.org/10.1016/j.scriptamat.2009.12.033.

[15] L. Rokhlin, D. Eskin, Magnesium Alloys Containing Rare Earth Metals, CRC Press, London, 2003.

[16] D. Ando, Y. Ogawa, T. Suzuki, Y. Sutou, J. Koike, Age-hardening effect by phase transformation of high Sc containing Mg alloy, Mater. Lett. 161 (2015) 5–8, http://dx.doi.org/10.1016/j.matlet.2015.06.057.

[17] F. von Buch, J. Lietzau, B.L. Mordike, A. Pisch, R. Schmid-Fetzer, Development of Mg–Sc–Mn alloys, Mater. Sci. Eng. A 263 (1) (1999) 1–7, http://dx.doi.org/10.1016/S0921-5093(98)01040-5.

[18] C.J. Silva, Effect of Sc Addition on the Mechanical Properties of Mg-Sc Binary Alloys (Ph.D. thesis), McMaster University, 2014.

[19] C.J. Silva, A. Kula, R.K. Mishra, M. Niewczas, Mechanical properties of Mg-Sc binary alloys under compression, Mater. Sci. Eng. A 692 (2017) 199–213, http://dx.doi.org/10.1016/j.msea.2017.03.053.

[20] A.A. Nayeb-Hashemi, J.B. Clark, The Mg-Sc (Magnesium-Scandium) system, Bull. Alloy Phase Diagr. 7 (1986) http://dx.doi.org/10.1007/BF02869876.

[21] I. Polmear, Light Alloys: From Traditional Alloys to Nanocrystals, fourth ed., Butterworth-Heinemann, 2005.

[22] Y. Wu, W. Hu, Elastic and brittle properties of the B2-MgRE (RE=Sc, Y, Ce, Pr, Nd, Gd, Tb, Dy, Ho, Er) intermetallics, Eur. Phys. J. B 60 (1) (2007) 75–81, http://dx.doi.org/10.1140/epjb/e2007-00323-0.

[23] P.L.J. Conway, A.L. Shaw, L. Bassman, M. Ferry, K.J. Laws, Stabilisation of Disordered bcc Phases in Magnesium-Rare Earth Alloys, Springer International Publishing, Cham, 2017, http://dx.doi.org/10.1007/978-3-319-52392-7_68, Publication Title: Magnesium Technology.

[24] A.R. Natarajan, A. Van der Ven, First-principles investigation of phase stability in the Mg-Sc binary alloy, Phys. Rev. B 95 (21) (2017) 214107, http://dx.doi.org/10.1103/PhysRevB.95.214107.

[25] A. Issa, J.E. Saal, C. Wolverton, Formation of high-strength β' precipitates in Mg–RE alloys: The role of the Mg/β'' interfacial instability, Acta Mater. 83 (Supplement C) (2015) 75–83, http://dx.doi.org/10.1016/j.actamat.2014.09.024.

[26] A. Zunger, S.-H. Wei, L.G. Ferreira, J.E. Bernard, Special quasirandom structures, Phys. Rev. Lett. 65 (3) (1990) 353–356, http://dx.doi.org/10.1103/PhysRevLett.65.353.

[27] B.L. Gyorffy, Coherent-potential approximation for a nonoverlapping-muffin-tin-potential model of random substitutional alloys, Phys. Rev. B 5 (6) (1972) 2382–2384, http://dx.doi.org/10.1103/PhysRevB.5.2382.

[28] C. Jiang, B.P. Uberuaga, Efficient ab initio modeling of random multicomponent alloys, Phys. Rev. Lett. 116 (10) (2016) 105501, http://dx.doi.org/10.1103/PhysRevLett.116.105501.

[29] A. van de Walle, M. Asta, Self-driven lattice-model Monte Carlo simulations of alloy thermodynamic properties and phase diagrams, Modelling Simulation Mater. Sci. Eng. 10 (5) (2002) 521, http://dx.doi.org/10.1088/0965-0393/10/5/304.

[30] J.W.D. Connolly, A.R. Williams, Density-functional theory applied to phase transformations in transition-metal alloys, Phys. Rev. B 27 (8) (1983) 5169–5172, http://dx.doi.org/10.1103/PhysRevB.27.5169.

[31] G. Kresse, J. Furthmüller, Efficiency of ab-initio total energy calculations for metals and semiconductors using a plane-wave basis set, Comput. Mater. Sci. 6 (1) (1996) 15–50, http://dx.doi.org/10.1016/0927-0256(96)00008-0.

[32] G. Kresse, J. Furthmüller, Efficient iterative schemes for ab initio total-energy calculations using a plane-wave basis set, Phys. Rev. B 54 (16) (1996) 11169, http://dx.doi.org/10.1103/PhysRevB.54.11169, Publisher: APS.

[33] J.P. Perdew, K. Burke, M. Ernzerhof, Generalized gradient approximation made simple, Phys. Rev. Lett. 77 (18) (1996) 3865–3868, http://dx.doi.org/10.1103/PhysRevLett.77.3865.

[34] G. Kresse, D. Joubert, From ultrasoft pseudopotentials to the projector augmented-wave method, Phys. Rev. B 59 (3) (1999) 1758, http://dx.doi.org/10.1103/PhysRevB.59.1758, Publisher: APS.

[35] H.J. Monkhorst, J.D. Pack, Special points for Brillouin-zone integrations, Phys. Rev. B 13 (12) (1976) 5188, http://dx.doi.org/10.1103/PhysRevB.13.5188, Publisher: APS.

[36] A. van de Walle, M.D. Asta, G. Ceder, The alloy theoretic automated toolkit: A user guide, CALPHAD 26 (2002) 539–553, http://dx.doi.org/10.1016/S0364-5916(02)80006-2.

[37] A. van de Walle, Multicomponent multisublattice alloys, nonconfigurational entropy and other additions to the Alloy Theoretic Automated Toolkit, CALPHAD 33 (2009) 266–278, http://dx.doi.org/10.1016/j.calphad.2008.12.005.

[38] A. Natarajan, A. Van der Ven, Linking electronic structure calculations to generalized stacking fault energies in multicomponent alloys, npj Comput. Mater. 6 (2020) http://dx.doi.org/10.1038/s41524-020-0348-z.

[39] P. Conway, Structure and Stability of New Types of Lightweight High Entropy and Compositionally Complex Alloys (Ph.D. thesis), UNSW Sydney, 2018.